

OPTICAL CONSTANTS OF BRUSH ELECTRODEPOSITED CuInTe₂ FILMS

P. MUTHUSAMY^a, A. PANNEERSELVAM^{b,*}

^aAnna University, Research scholar, Chennai – 600 025

^bDepartment of Physics, Paavai Engineering College, Pachal – 637 018

Electrodeposition method has been used to deposit of CuInTe₂ thin films on transparent glass substrate with thickness range from 200 to 400 nm at various temperatures ranging from 30° to 80°C by using the brush. UV visible spectrometer was used to record the transmission spectra of CuInTe₂ thin films in the wavelength range between 900 to 1800 nm. It is revealed that the optical energy gap (E_g) is increased from 0.96 eV to 1.01 eV when the substrate temperature decreases. The variation in refractive index and extinction coefficient with photon energy were studied and material properties such as dielectric constant, plasma frequency, and carrier density to effective mass, dispersion, oscillator energy and optical moments were estimated.

(Received March 10, 2019; Accepted May 30, 2019)

Keywords: Semiconductor, Thin films, Electronic material, Optical properties

1. Introduction

CuInTe₂ (CIT) is a novel material for solar energy application due to the following characteristics such as absorption co-efficient, near infrared band gap, non linear susceptibility [1, 2]. This material could have large tolerance to stoichiometry condition when compared to other ternary and binary compounds [3]. CIT thin films have been deposited by many methods such as slow thermal evaporation [4], spin coating [5], calcination of stacked elemental layers [6] and co-evaporation of elements [7], pulsed laser deposition [8], electro-deposition [9], pulse plating [10] and brush plating method [11]. Amongst all the methods, the brush plating technique is a good and simple method thin film deposition. It is an effective and cost effective.

Brush plating can be called as particular plating or swab plating technique. It is an extremely helpful and simple method for contact plating. In its least complex shape, the brush plating process seems to be painting. Brush plating gear contains control packs, solutions, plating instruments, anode spreads, and assistant hardware. The power pack has two leads. One is corresponded with the plating instrument and the other is corresponded with the workpiece to be plated. The anode consists of a material which holds the necessary arrangement. The plate can be dipped in the solution and followed by the brushes against to the surface of the workpiece that will be done. At the particular point, the anode touches the work surface so as to frame the circuit and finally electrodeposition is produced. Plating occurs just when the anode contacts the workpiece. Besides the brush plating process and the plating instrument is fixed firmly in movement at whatever point it contacts with the work surface.

Therefore, in this work, CIT films were brush plated on tin oxide coated glass substrates in the (5 ohms sq). The complete procedure of depositing CIT films is explained in the literature [11]. In our previous work, results were obtained on CIT films deposited for 20 min [11]. In this work on the optical properties of CIT films deposited for 10 min at various substrate temperatures is reported and discussed. Finally optical constants were also established from the optical studies. The authors were attempted to obtain result and deposited.

*Corresponding author: panneer.phy@gmail.com

2. Experimental methods

CIT films were brush plated for 10 min at different substrate temperatures ranging from 30 - 80°C with thickness of 1.0 μm [11]. Thickness of the prepared thin film studies by Mitutoyo surface profilometer in the range between 200 nm to 400 nm. The films were studied using X-ray diffraction and optical properties such as band gap also estimated by using Hitachi U3400 UV-VIS-NIR spectrophotometer. XRD technique was used to analyze the crystal structure by using PANalytical X'Pert Pro Diffractometer with sifted $\text{CuK}\alpha$ radiation source.

3. Results and discussion

Fig.3.1 shows the XRD Pattern of the deposited CIT thin films deposited at various substrate temperatures. The deposited films were polycrystalline in nature with prominent peaks namely (112), (204/220) and (116/312) planes. These are attributed to the CIT thin films. This is well agree with the JCPDS card No.10-0421. The peak intensity was increased and peak width was narrowed due to increase in the substrate temperature. As the substrate temperature expanded, the intensity of the peaks expanded and the width of the peaks were diminished. The crystallite size can be calculated from the Scherrer's equation.

$$\text{Crystalline Size (D)} = \frac{0.95\lambda}{\beta \cos \theta} \quad (1)$$

where, λ is the wavelength of X-rays, β is the full width half maximum, θ is the diffraction angle. The crystallite size of the prepared CIT thin films were found to be from 10 nm to 40 nm as the substrate temperature increased from 30°C to 80°C. Fig.3.2 reveals the transmission spectra of the CIT films maintained at various substrate temperatures. The spectra produce interference fringes and the refractive index of the CIT thin film estimated by the envelope strategy [12] as follows,

$$n = [N + (N^2 - n_s^2)]^2 \quad (2)$$

$$N = \frac{(n_s^2 + 1)}{2} + 2n_s \frac{(T_{\max} - T_{\min})}{T_{\max} T_{\min}} \quad (3)$$

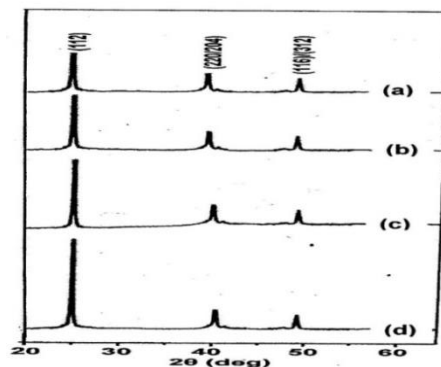


Fig.3.1. X-ray diffraction profile of CIT films deposited at different substrate temperatures (a) 30°C (b) 50°C (c) 70°C (d) 80°C.

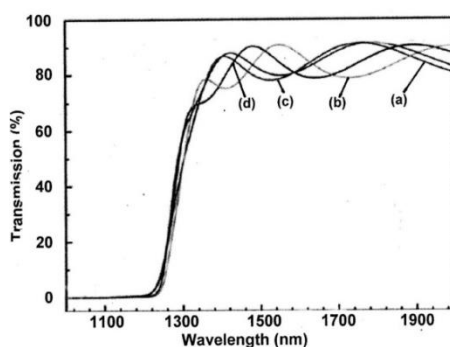


Fig.3.2. Transmission spectra of CIT films deposited at different substrate temperatures (a)80°C (b) 70°C (c) 50°C (d) 30°C.

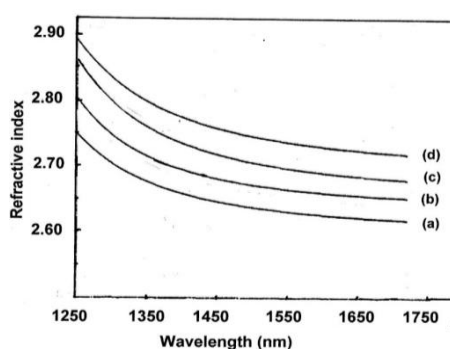


Fig.3.3. Variation in Refractive index with wavelength for the prepared CIT films Deposited at different substrate temperatures (a) 30°C (b) 50°C (c) 70°C (d) 80°C.

where n_s is the refractive index of the substrate, T_{\max} and T_{\min} are indicating the maximum and minimum transmittances at a very similar wavelength in the fitted envelope curve on a transmittance peak. The refractive index of the CIT thin films were found to be from 2.75 to 2.89 at 1250 nm wavelength as the substrate temperature is increased.

The estimation of the refractive record computed from the above conditions was in the scope of 2.75 – 2.89 at 1250 nm with increment of substrate temperature (Fig.3.3). The result indicating that the value of refractive index is decreased with increases of wavelength. These are well agree with the reported literature [6]. The refractive index diminishes with increment of wavelength. The esteem agrees with prior report [6]. The calculated of the absorption co-efficient (α) was ascertained utilizing the connection.

$$\alpha = \frac{1}{d} \ln \left\{ \frac{(n-1)(n-n_s)}{(n+1)(n-n_s)} \right\} \left[\frac{\left(\frac{T_{\max}}{T_{\min}} \right)^2 + 1}{\left(\frac{T_{\max}}{T_{\min}} \right)^2 - 1} \right] \quad (4)$$

where 'd' is the thickness of the thin film and alternate parameters have the importance as given in equation(4). Optical absorption peaks were recorded on the film maintained at various substrate temperatures. The prepared CIT thin films show a high absorption coefficient in the order of 104 cm^{-1} . Fig.3.4 shows the curve plotted between $(\alpha h\nu)^2$ and $h\nu$. It displays the linear behaviour in band edge, the band gap of the CIT films also were recorded to be in the range of 0.965 – 1.01 eV.

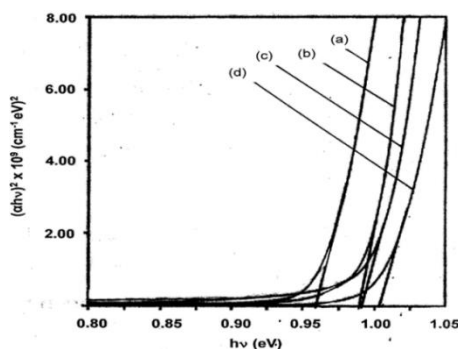


Fig.3.4. Tauc's plot of CIT films at different substrate temperatures (a) 80°C (b) 70°C (c) 50°C (d) 30°C.

The band gap gradually increases with decrease of substrate temperature, due to the small crystalline size. In Previous literature, it is reported that band gap values is 0.86 – 0.98 eV for the CIT thin films synthesized by other methods. The band gap of CIT in thin film prepared by other technique was in the range of 0.86 – 0.98 eV [6].

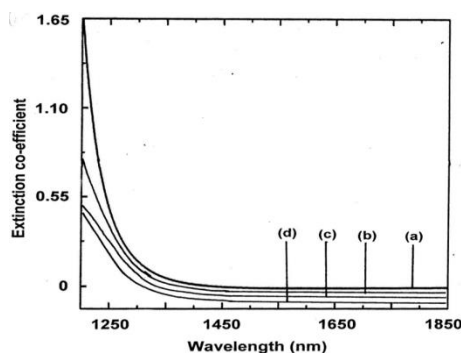


Fig. 3.5. Variation in Extinction co-efficient with wavelength for prepared CIT films at different substrate temperatures (a) 30°C (b) 50°C (c) 70°C (d) 80°C.

The following relation used to find the Extinction coefficient from the absorption coefficient.

$$K = \frac{\alpha\lambda}{4\pi} \quad (5)$$

where, α is the absorption coefficient and λ is the incident wavelength. As shown in the figure, the extinction constant decreases with increase in the wavelength. On contrary the decrease in extinction coefficient with increase of wavelength reveals that the fraction of light lost due to decrease in scattering and absorbance. A basic intrinsic property of the material is the dielectric constant. The real part of dielectric constant shows percentage of absorption energy slow down the speed of light, whereas the imaginary part shows absorbs energy of electrical field due to dipole motion. The study of the real and half of imaginary part of a complex number of the dielectric constant explains information regarding the dielectric loss issue which the ratio of the imaginary part to the real part of the dielectric constant. The real and the imaginary parts of the dielectric constant can be calculated using the following equation [12].

$$\epsilon_1 = n^2 - k^2 \text{ and } \epsilon_2 = 2nk \quad (6)$$

The phenomenon of reflectivity of a semiconducting material within the infrared region shows abnormal dispersion as the incident photon energy reaches the corresponding value of plasma wavelength λ_p . When $n_2 \gg k_2$ and $\omega T < 1$, the dielectric constant is given as [13].

$$\epsilon_1 = \epsilon_\infty - \frac{[\epsilon_\infty \omega_p^2]}{\omega^2} \quad (7)$$

where, ϵ_∞ is the limiting value of the dielectric constant of the materials, Variation in ϵ_2 with $1/\omega_2$ for CIT films deposited at various substrate temperatures is shown in Fig.3.6. Plasma frequency ω_p and ϵ_∞ were estimated from the slope and intercept of the linear portion of the ϵ_1 versus $1/\omega_2$ plot. The values of ϵ_∞ and ω_p values are tabulated in Table 3.1. In transparent region, the relation between the optical dielectric constant (ϵ_1), the wavelength (λ), and also the ratio, n , is given by the following relation [14].

$$\epsilon_1 = n^2 = \epsilon_L - D\lambda^2 \quad (8)$$

where, ϵ_1 is the real part of dielectric constant, ϵ_L is the lattice dielectric constant and D is a constant depending on the ratio of carrier density. The concentration to the effective mass is given by this equation.

$$\epsilon_1 = n^2 = \epsilon_L - D\lambda^2 \quad (9)$$

where, 'e' is that the charge of the electron, N is the free charge carrier concentration (ϵ_0) is the permittivity of free space, m^* is the effective mass of the hole and c is that the velocity of flight [15]. Fig.3.7 shows the relation between n_2 and λ_2 for the prepared CIT thin films deposited at various substrate temperatures. It is found that the dependence $\epsilon_1 (= n_2)$, on λ_2 is linear.

This linear part of this dependence to zero wavelength offers the value of ϵ_L by preparing. From the slope of this linear part, the constant D can be calculated, from that the value (N/m^*) for the prepared thin films is obtained (Table-3.1).

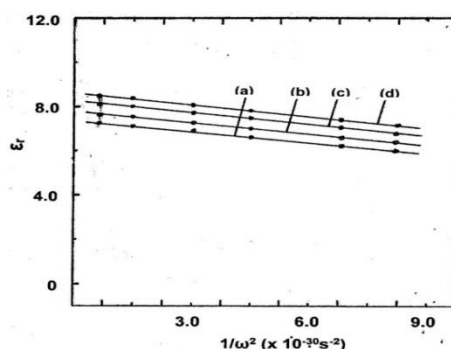


Fig.3.6. Variation in real part of dielectric constant with wavelength for the prepared CIT films Deposited at different substrate temperatures (a) 30°C (b) 50°C (c) 70°C (d) 80°C.

The Wemple and DiDomenico have proposed a single effective oscillator model [16], The optical properties can be calculated by extrapolating following approximation by the equation.

$$n^2 - 1 = \frac{(E_d E_0)}{(E_0^2 - E^2)} \quad (10)$$

where, $E = h\nu$ is the photon energy, n is the refractive index, E_0 is the single-effective oscillator energy and E_d is the dispersion energy that can be measured the

average strength of the interband optical transitions. Plotting curve $(n_2 - 1)^{-1}$ against E_2 provides the oscillator parameters by fitting a straight linear line. Fig. 3.8 shows the plot of $(n_2 - 1)^{-1}$ vs E_2 for the films deposited at different substrate temperatures. The slope (E_0/E_d) is used to estimated the value of E_0 and therefore the intercept on the vertical axis E_0/E_d also can be found. The values of the static refractive index (n_0) can be measured by analyzing the Wemple–Di Domenico dispersion equation (10) to $E \rightarrow 0$. The estimated values of n_0 are 2.65, 2.68, 2.72 and 2.76 for the prepared films deposited at various substrate temperatures.

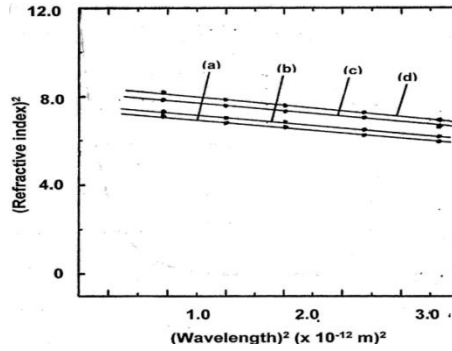


Fig.3.7. Variation in square of refractive index with square of wavelength for prepared CIT films deposited at different substrate temperatures (a) 30°C (b) 50°C (c) 70°C (d) 80°C.

The calculated values of n_0 , E_0 and E_D are listed and tabulated in additionally, the optical band gap (E_g) was determined from the Wemple–Di Domenico dispersion parameter E_0 using the relation $E_g = E_0/1.4$. The calculated energy gap values are found to be 0.96, 0.98 and 1.01 electron volt for the prepared CIT thin films for the different substrate temperatures. It is well agreement with the value estimated from Tauc’s plot.

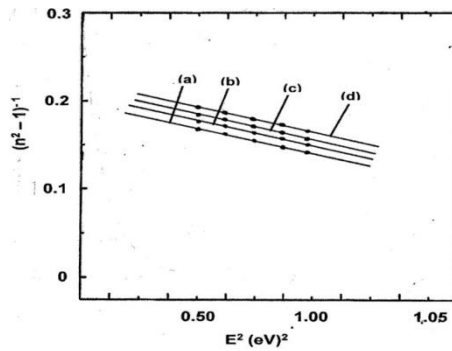


Fig.3.8. Variation of $(n_2 - 1)^{-1}$ against E_2 plot for the prepared CIT films deposited at different substrate temperatures (a) 30°C (b) 50°C (c) 70°C (d) 80°C.

M_{-1} and M_{-3} are corresponded to the Moments of the Optical Spectra for the CIT thin films. These are obtained from the following relations [17],

$$E_0^2 = \frac{M_{-1}}{M_{-3}} \tag{11}$$

$$E_0^2 = \frac{M_{-1}^3}{M_{-3}} \tag{12}$$

The single-oscillator parameters such as E_o and E_d are associated to the imaginary component ϵ_i of the complex dielectric constant. Thus, finding the moments is playing role in very vital developing optical devices of the optical material. The estimated values also are tabulated in Table 3.1. The obtained result result show that M_{-1} and M_{-3} moments decreased with increase of substrate temperatures.

Table 3.1. Calculated Band gap, refractive index, plasma frequency, Oscillator energy, dispersion energy, optical moments of CIT films deposited at different substrate temperatures are tabulated.

Subs. Temp. (°C)	n_o	E_g (eV)	E_o (eV)	E_d (eV)	ϵ_∞	ω_p	M_{-1}	M_{-3}
30	2.65	0.96	1.35	6.05	7.5	3.73	5.26	2.89
50	2.68	0.98	1.37	6.37	7.9	3.55	4.76	2.54
70	2.72	0.982	1.373	6.52	8.1	3.51	4.65	2.49
80	2.76	1.01	1.41	7.42	8.3	3.47	4.44	2.23

4. Conclusions

CuInTe₂ thin films 0.96 eV to 1.01 eV were successfully prepared by using brush plating technique. Transmission spectra were recorded for the CIT films and shown interference fringes. Optical constants like index of refraction, band gap, extinction co-efficient, dispersion energy, oscillator energy, and ratio of carrier concentration to effective mass, plasma frequency, limiting value of dielectric constant, optical moments were estimated. The variation in index of refraction and extinction co-efficient with wavelength were calculated. Band gap values obtained from Tauc's plot fitted well with analysis of the oscillator model.

References

- [1] L.L.Kazmerski, Renew Sust.EnergyRev.**1**, 71(1997).
- [2] D.Xue,K.Betzler,H.Hesse,Phys.Rev.B**62**, 3546 (2000).
- [3] S.Siebritt,U.Rau(Eds.),Wide-GapChalcopyrites,Springer,Berlin,2006s.
- [4] L.L.Kazmerski,Y.J.Juang, J.Vac.Sci.Technol.**14**, 769 (1977).
- [5] M.Boustani, K.E.Assali, T.Bekay, E.Ech-Chamikh, A.Outzourhit, A.Khiara, L. Dreesen, Semicond. Sci.Technol. **12**, 1658(1997).
- [6] S.Roy, P.Guha, S.Chaudhuri, A.K.Pal, Vacuum **65**, 27 (2002).
- [7] S.Roy, B.Bhattacharjee, S.N.Kundu, S.Chaudhuri, A.K.Pal, Mater.Chem.Phys.**77**, 365 (2002).
- [8] V.F.Gremenok, I.A.Victorov. I.V.Bodnar, A.E.Hill, R.D.Pilkington, R.D. Tomlinson, M.V.Yakushev, Mater.Lett.**35**, 130 (1988).
- [9] Solar Energy Materials & Solar Cells **91**, 621 (2007).
- [10] K.R.Murali, C.Vinodhini, K.Srinivasan, Mater.Sci.Semicond.Processing **15**, 194 (2012).
- [11] K.R.Murali, P.Muthusamy, A.Panneerselvam, J.Mater.Sci. Mater in Electronics **24**, 3412 (2013).
- [12] W.W. Hou, B.Bob, S.Li, Y.Yang, Thin Solid Films**517**,6853 (2009).
- [13] H.A. Lyder,Phys.Rev. **134A**, 106 (1964).
- [14] P.O.Edward, Hand Book of Optical Constants of Solids, Academic Press, NewYork1985. P265.
- [15] S. H. Wemple, M.DiDomenico, Phys. Rev. B **3**, 1338 (1971).
- [16] M.S.Kim,K.G.Yim, J.Son, J.Y.Leem, Bull.Kor.Chem. Soc.**33**, 1235 (2012).
- [17] J.N. Zeng, J.K. Low, Z.M. Ren, T. Liaw, Y.F. Lu, Appl. Surf. Sci. **197–198**, 362 (2002).